Electronic Supplementary Material (ESI) for Nanoscale.
This journal is © The Royal Society of Chemistry 2023

SUPPORTING INFORMATION

FeAu mixing for high-temperature control of light scattering at the nanometer scale

Anna V. Nominé,[a†] Ekaterina V. Gunina,[b†] Semyon V. Bachinin,[b] Alexander I. Solomonov,[b] Mikhail V. Rybin,[b] Sergey A. Shipilovskih,[b] Salah-Eddine Benrazzouq,[a] Jaafar Ghanbaja,[a] Thomas Gries,[a] Stephanie Bruyère,[a] Alexandre Nominé,[a,c,d] Thierry Belmonte,[a*] Valentin A. Milichko[a,b*]

Part I. Experimental Methods

PVD Deposition: FeAu films have been deposited on pre-cleaned substrates by DC magnetron co-sputtering from two metallic targets: iron target (50 mm in diameter, 0.25 mm thick, 99.5% purity) and gold target (50 mm in diameter, 3 mm thick, 99.9% purity). Quartz and Si wafers were used as substrates for laser ablation and plasma treatment, respectively. Two independent magnetrons (Figure S2) connected to independent DC current generators allow the simultaneous deposition of two different metals from 2 sputtering targets (composite targets can also be used to increase the number of deposited elements). The magnetrons focused on the center of the substrate holder and inclined by 30 degrees with respect to the substrate normal were used. During the deposition, the sample holder is rotated at 26 rpm to ensure the homogeneity of the deposition. Target to substrate distance was set to 10 cm. The base pressure in the sputtering chamber during deposition was 0.58 Pa in an atmosphere containing 10 vol% H_2 and 90 vol% Ar. The compositions of the thin films were controlled by the adjustment of the power applied to metallic target and stoichiometric FeAu films were obtained at 120 W on Fe target and 40 W on Au target, respectively (Figure S2c). Before the film deposition, a shutter was placed in front of the target to isolate the substrate during 2 min in order to remove native oxide layers. The thickness was controlled by adjusting the sputtering time. Thin films were deposited without external heating and the deposition temperatures were below 50 °C.

The layer thickness was determined as an average value of 10 measurements (Figure S3) carried out on profilometer Dektak XT Bruker Nano GmbH, Germany, while the atomic elemental composition of the deposited films was verified on a SEM Zeiss Gemini 500 with an Oxford X-Max EDS-SDD detector with a real active surface of 80 mm² which are 56 at.% of Au and 44 at.% of Fe (Table S1).

Laser ablation: FeAu NPs have been produced from the FeAu film on a glass. The fabrication of the NPs has been done by laser ablation (Figure S5) with femtosecond system (Light Conversion Pharos: 200 fs pulse duration, 1030 nm operating wavelength, 1 MHz repetition frequency, 10 W average power, 10 μJ pulse energy). The ablation took place in a chamber (Figure S5) filled with N_2 or air. The laser radiation was focused by an objective Mitutoyo M Plan NIR VIS 50x/0.42NA. The obtained NPs then have been transferred to quartz substrate and TEM carbon grid for subsequent optical and electronic characterization.

TEM analysis: The *in situ* microstructural observations of synthesized NPs were carried out on a JEM-ARM 200F transmission electron microscope (JEOL Co., Japan) Cold FEG TEM/STEM operating at 200 kV and equipped with a spherical aberration (Cs) probe, image correctors (point resolution 0.12 nm in TEM mode and 0.078 nm in STEM mode), and EDS with JEOL Centurio detector (1 sr).

Optical characterization: To measure the optical scattering in a dark field geometry (Figure S6), the radiation from a white lamp (AvaLight-HAL-S-Mini Compact Halogen Light Source) was focused to the sample through an Mitutoyo M Plan APO 10x/0.28NA objective at an angle of 65 degrees. The scattering signal was collected through the upper Mitutoyo M Plan APO NIR 50×/0.42NA objective. For heating process, a femtosecond laser TEMA (150 fs pulse duration, 1047 nm operating wavelength, 80 MHz repetition frequency) was used. Further, the laser radiation passed through a harmonic generator (Avesta ATsG-O-W) to convert the incoming wavelength into the third harmonic (350 nm). This radiation was filtered by a laser-line filter and focused using Mitutoyo NUV 20×/0.42NA objective through the bottom optical channel.

Part II. Thin film fabrication

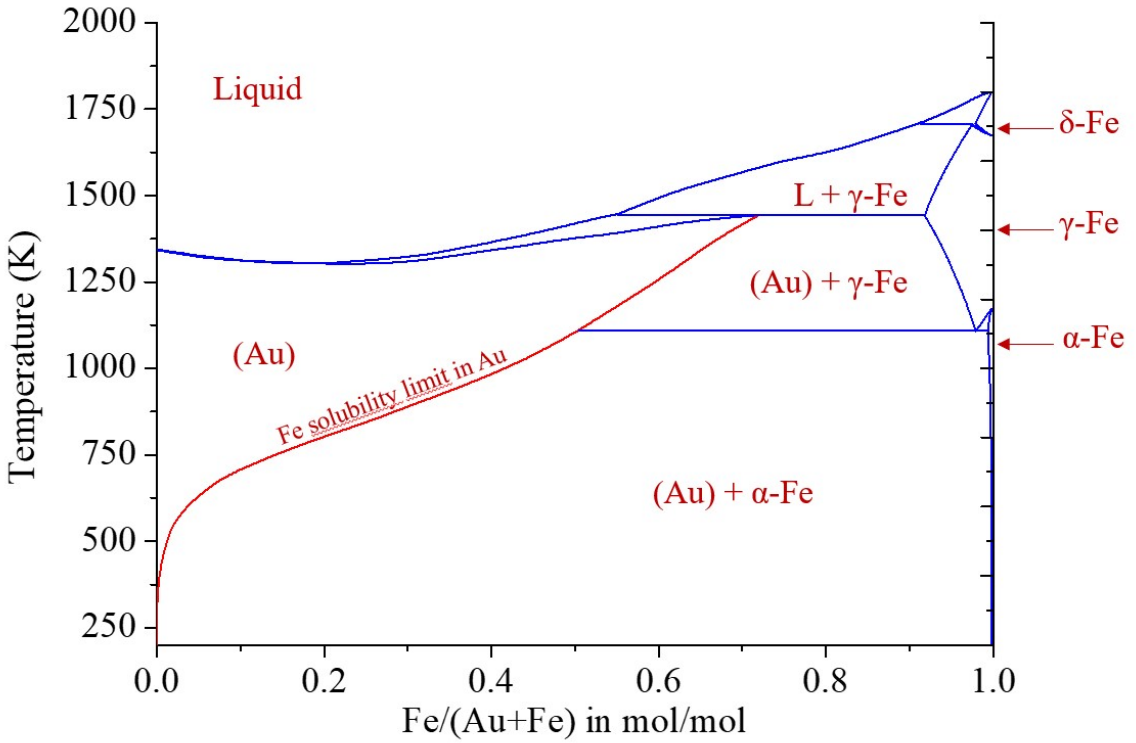

Figure S1. The Au–Fe phase diagram.

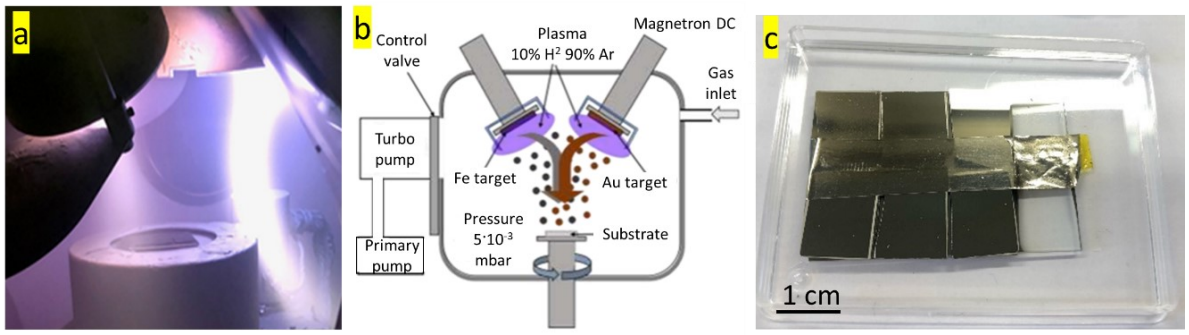

Figure S2. (a) Sputtering chamber during deposition process. (b) Schematic representation of PVD set up. (c) PVD co-deposited (Fe,Au) films on quartz substrates.

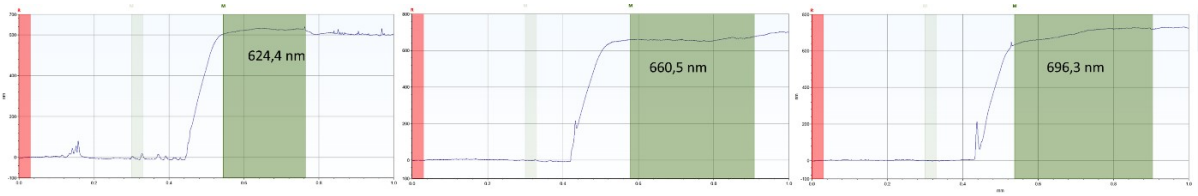

1	2	3	4	5	6	7	8	9	10	Δ
670,6	624,4	696,3	694,6	644,6	660,2	640,2	684,5	671,2	660,5	664,71 ± 40 nm

Figure S3. (Fe,Au) films thickness profilometry measurements.

Table S1. SEM EDS data of atomic elemental composition of *(*Fe,Au) film.

Spectrum: FeAu 1 (SEM analysis)

El AN Series	C norm. [wt.%]	C Atom. [at.%]	C Error (1 Sigma) [wt.%]
Au 79 L-series 87036	82	56	2,08
Fe 26 K-series 53634	18	44	0,49
Total:	100	100	

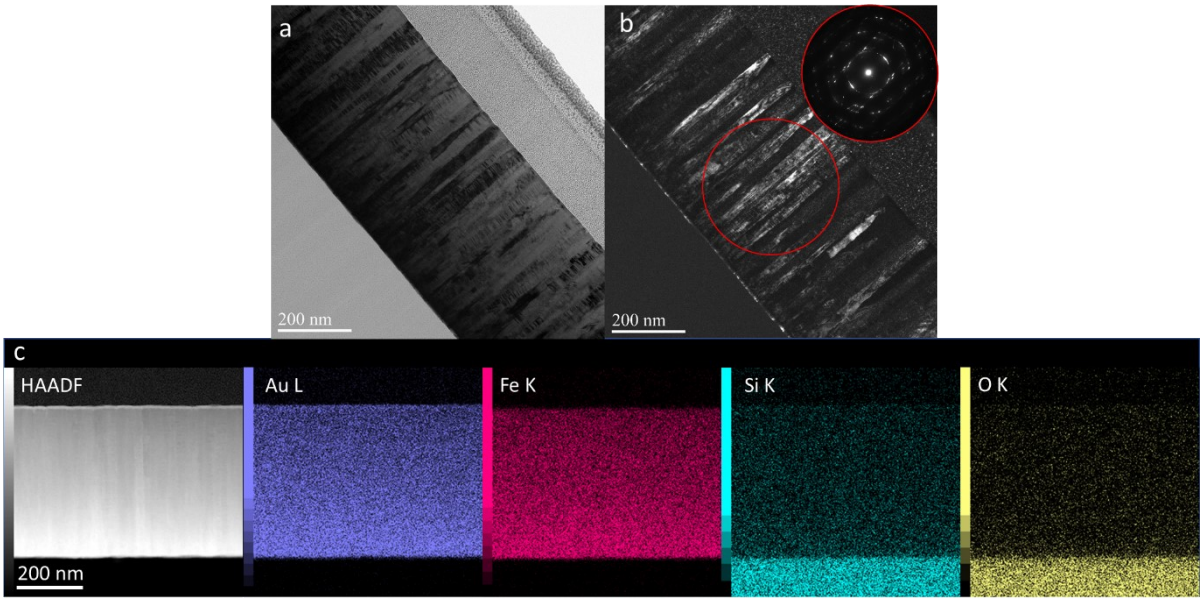

Figure S4. Cross-sectional TEM (a, b) and HAADF STEM image (c) with corresponding EDS elemental mapping of the PVD fabricated thin film on SiO_2 substrate FIB cross section. Inset in the DF TEM micrograph show selected area electron diffraction pattern of the region indicated by the red circle.

Part III. NP ablation and optical analysis

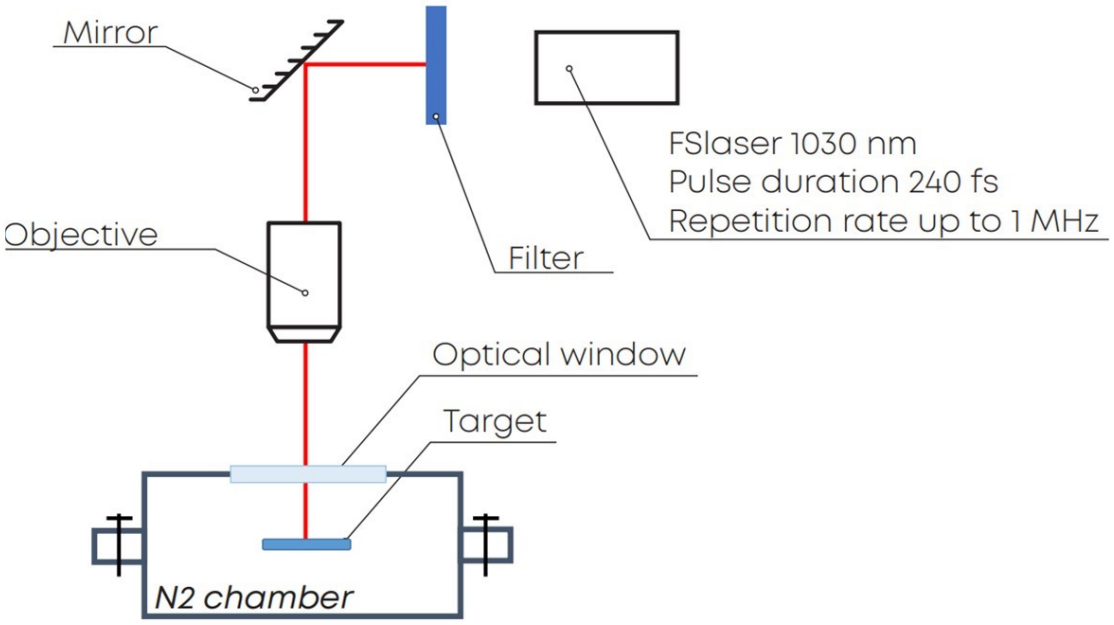

Figure S5. The scheme of the laser ablation of (Fe,Au) NPs in the chamber (N_2 or air atmosphere).

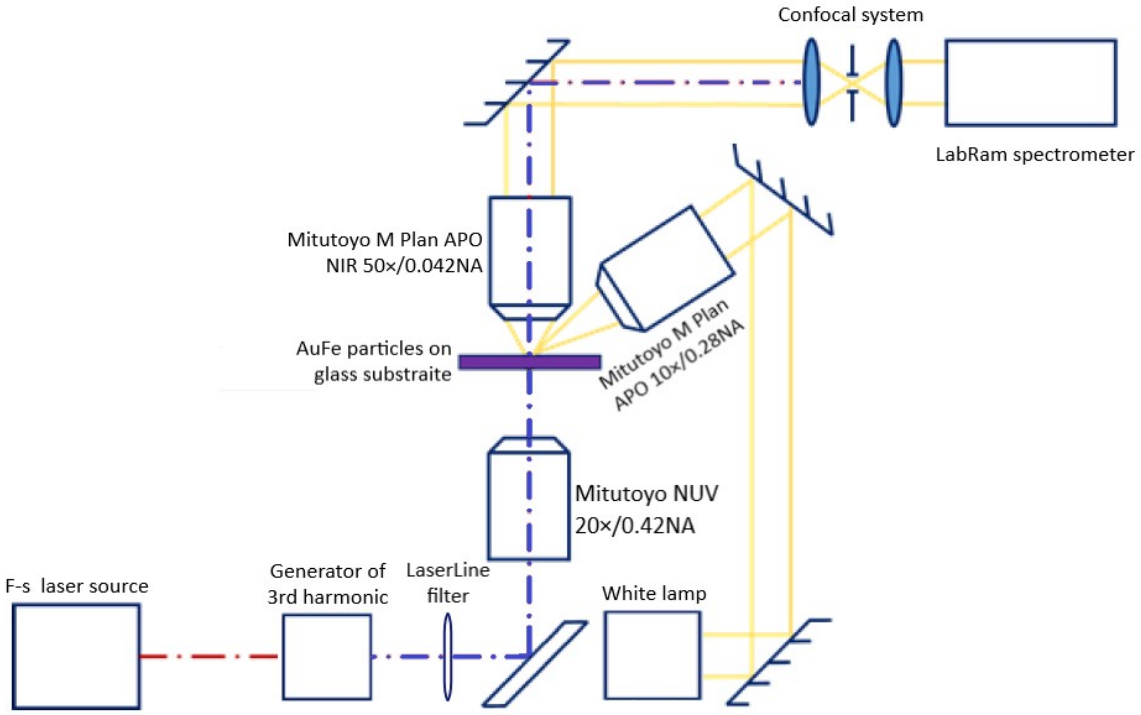

Figure S6. Experimental setup for optical characterization of single (Fe,Au) NPs.

Part IV. Electronic Discharges in Dielectric Liquid methods (EDDL) for the NPs synthesis

The experimental set-up used for the synthesis of NPs by discharges in liquid nitrogen is shown in Figure S7. A high voltage is delivered by a DC voltage power supply (Technix SR15-R-1200—15 kV— 80 mA) which feeds a high voltage solid-state switch (HTS-301-03-GSM). The switch is driven by a function generator that delivers a high voltage pulse instead of a DC voltage. The frequency, amplitude and the pulse width are applied to the power electrode (W pin). The second electrode (a PVD thin film on Si substrate) is connected to the ground and serves as cathode. The two electrodes are immersed in a 100 ml Dewar filled with liquid nitrogen. The inter-electrode gap distance is kept constant during the process by continuously adjusting it by micrometric screws. This enables breakdown, otherwise the process stops. The working electrode is a Tungsten wire of 1 mm in diameter, the grounded electrode is made of a thin film of iron and gold mixture (Fe,Au) deposited on Si wafer by PVD (Figure S7c). NPs were synthesized by erosion of the (Fe,Au) layers produced by co-sputtering, following parameters were applied: the high voltage pulse applied to the electrode is 5 kV, the pulse duration is 100 ns, the frequency of 10 Hz and the treatment duration of 30 min.

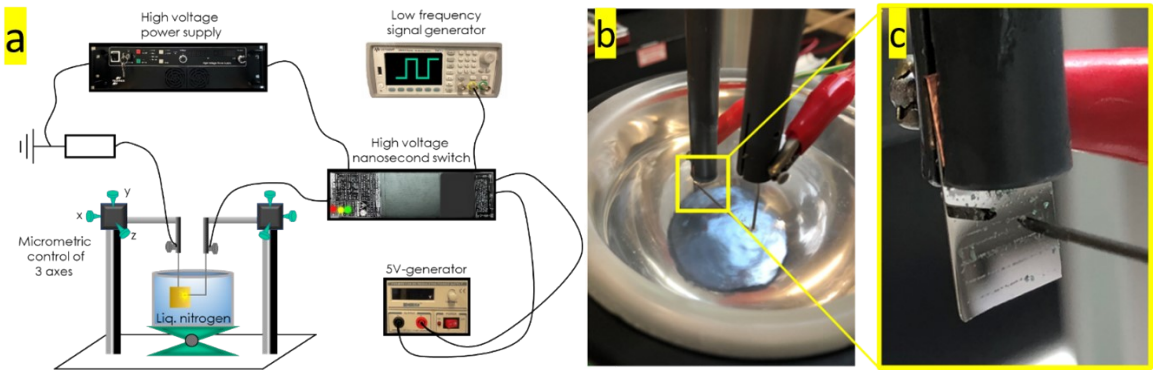

Figure S7. (a) Schematic representation of experimental set up of EDDL process. (b) Image of the electrodes during the experiment and (c) the electrodes after the treatment.

Part V. TEM analysis

Table S2. Composition of (Fe,Au) NPs obtained by laser ablation in N_2 and air atmosphere and by EDDL process (Part IV).

Element	**Laser ablation in air (at.%)**	**Laser ablation in N_2 (at.%)**	**EDDL**
O K	36	13	17
Fe K	14	30	33
Au M	50	57	45
Si K	0	0	5
Total	100	100	100

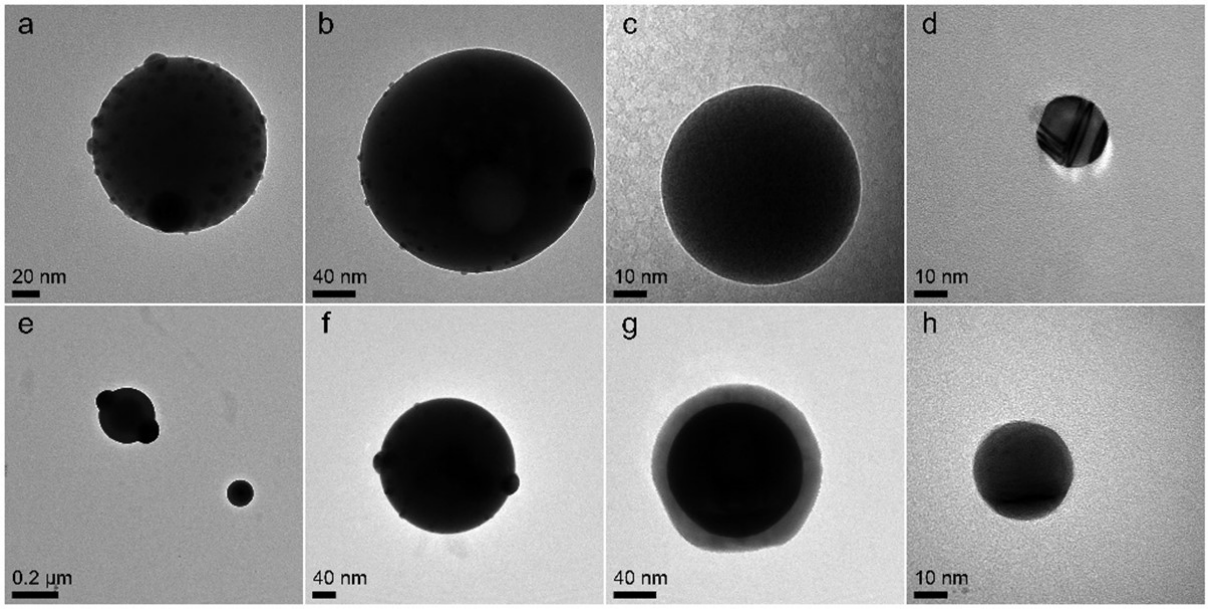

Figure S8. TEM micrographs of the NPs obtained by laser ablation of (Fe,Au) film in N_2 (a-d) and air (e-h) atmosphere.

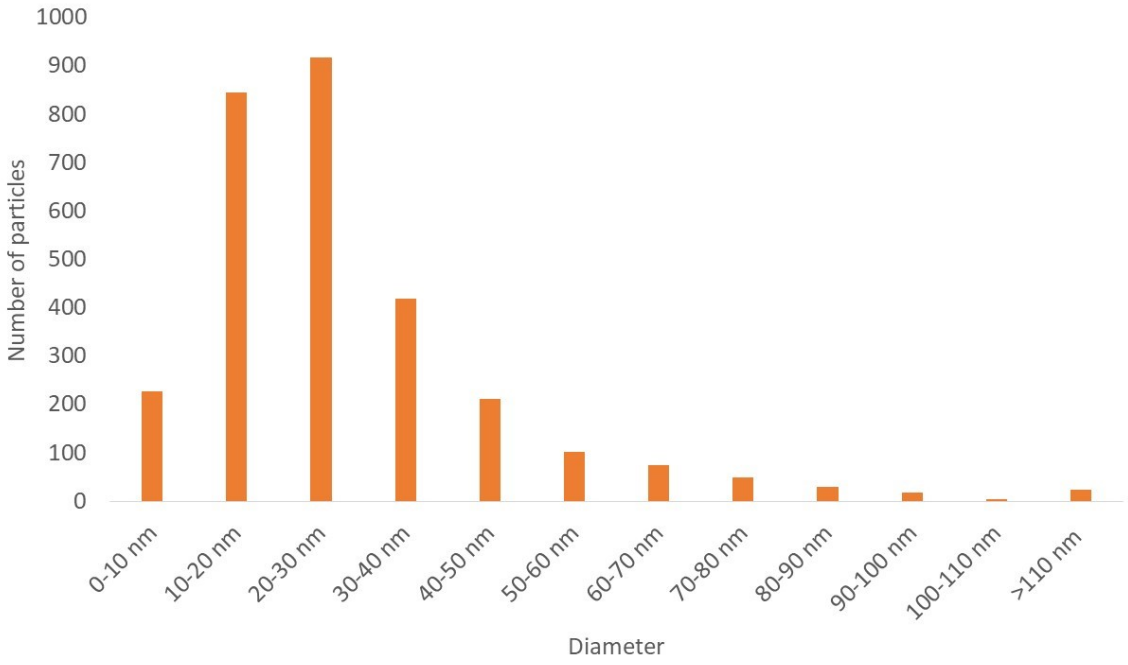

Figure S9. Size distribution of (Fe,Au) NPs obtained by laser ablation in N_2 correlating with that of the NPs obtained by EDDL.

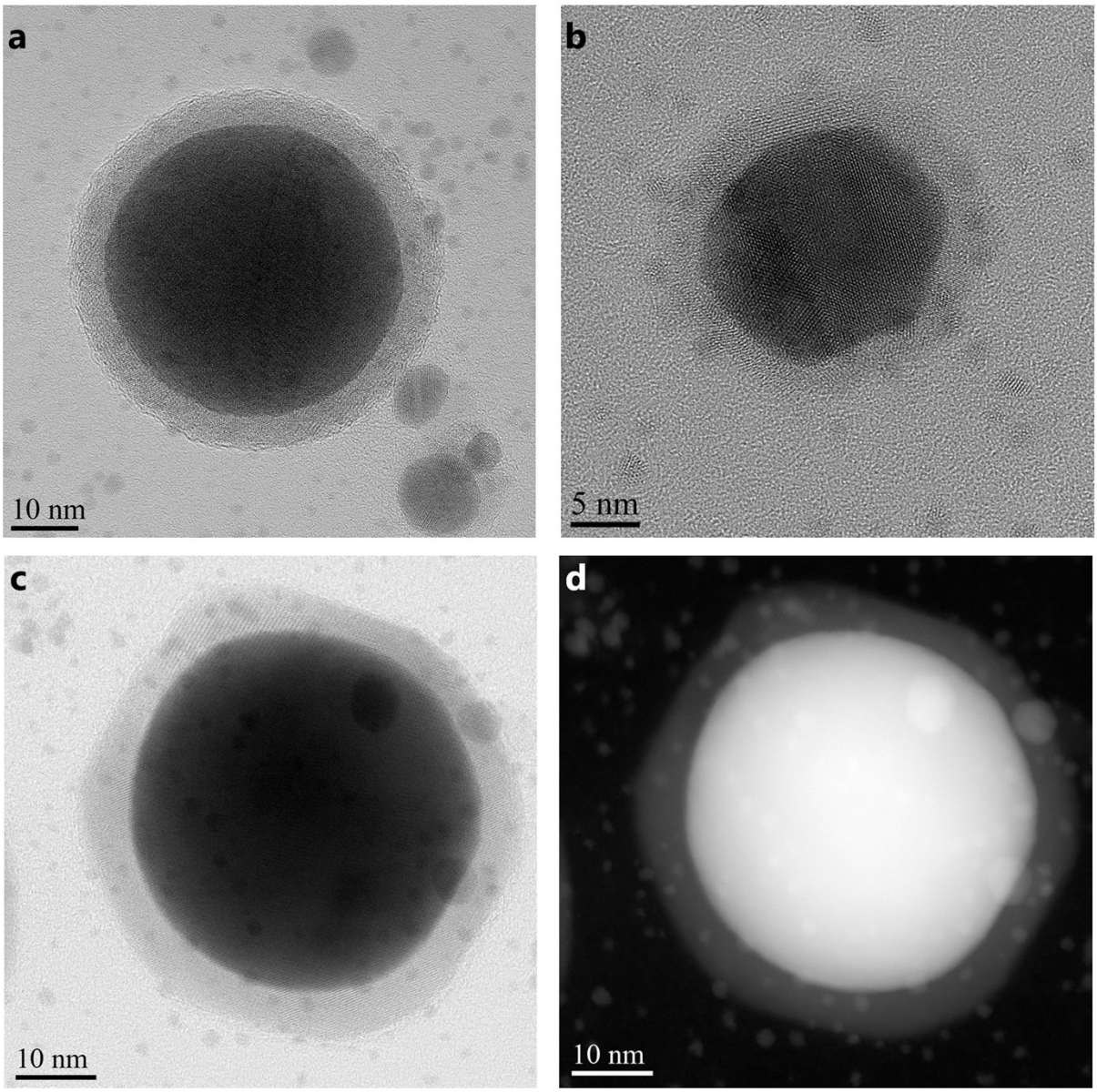

Figure S10. Example of (Fe,Au) NPs obtained by laser ablation in air atmosphere. (a,b) HRTEM micrographs of (Fe,Au) NPs. (c-d) BF and HAADF HR STEM micrographs of smaller nanoparticles showing a good crystallinity.

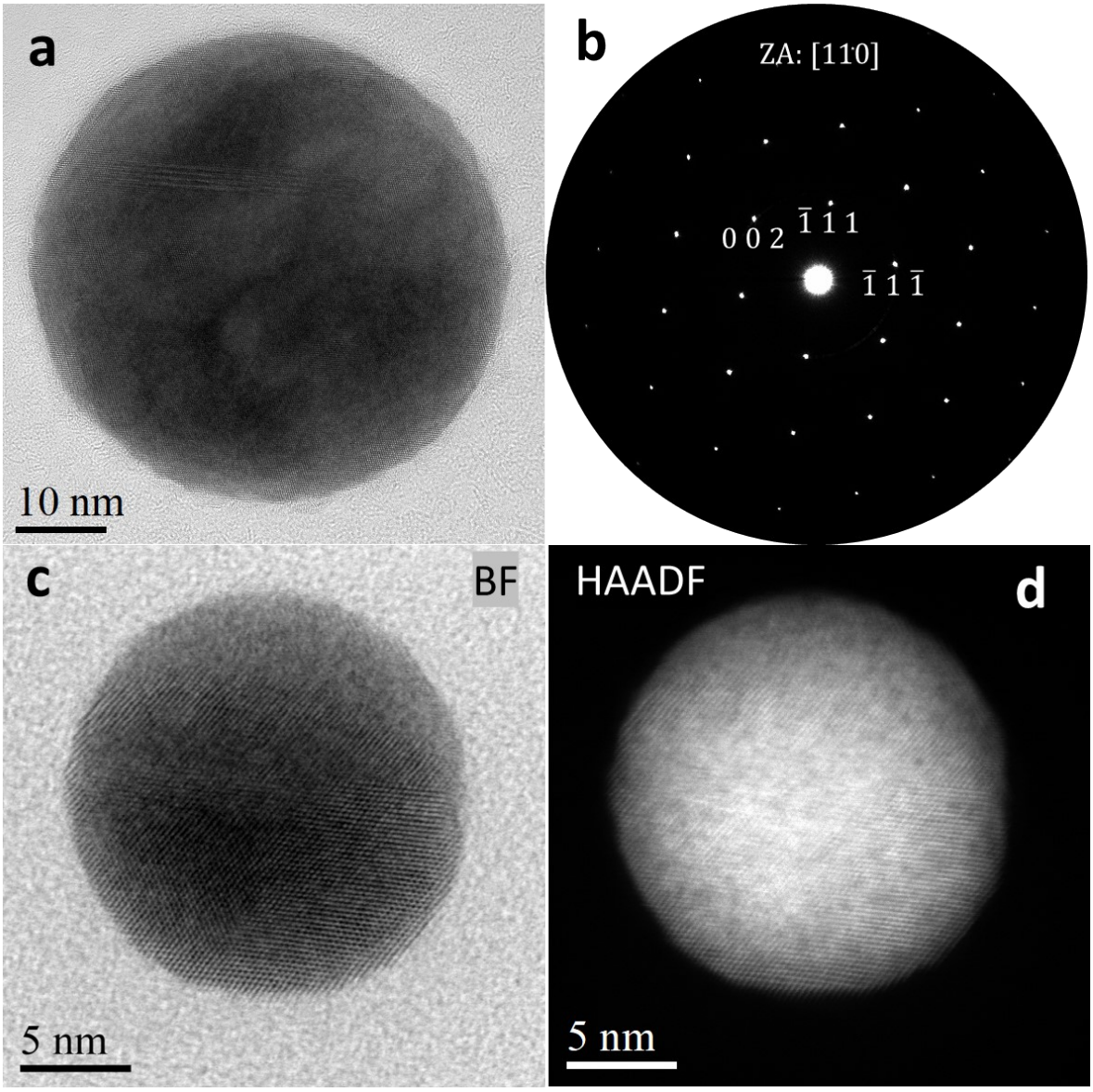

Figure S11. Example of (Fe,Au) NPs obtained by laser ablation in N_2 atmosphere. (a) HRTEM micrographs of (Fe,Au) NP with b) his corresponding SAED pattern. (c-d) BF and HAADF HR STEM micrographs of smaller nanoparticles showing a good crystallinity. The SAED pattern demonstrates that diffraction spots indexed to the (-1 1 -1), (-1 1 1) and (002) reflections with zone axis [110], suggesting that AuFe nanoparticle is a well-defined single crystal that can be associated to the $Au_{50}Fe_{50}$.

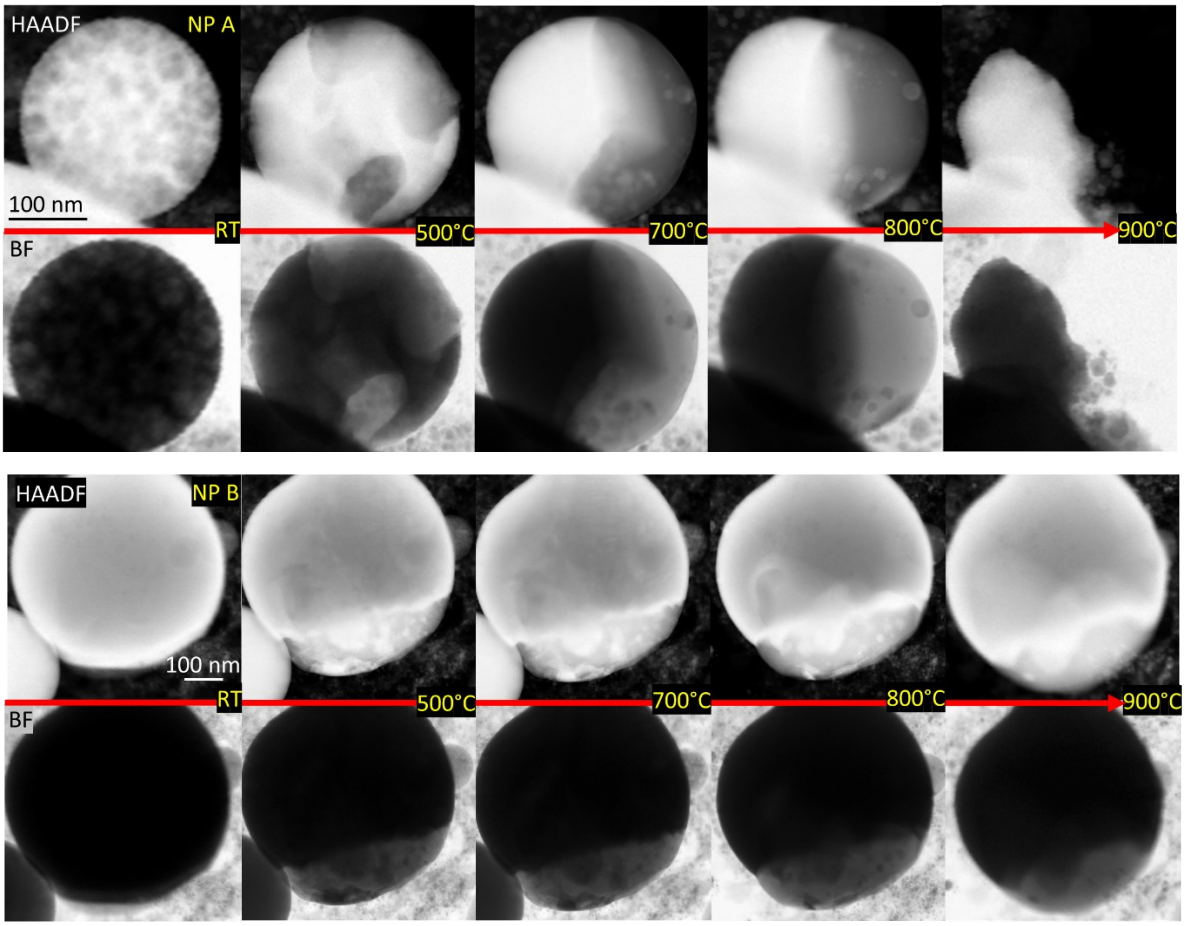

Figure S12. HAADF and BF STEM images showing the structure evolution of two selected (Fe,Au) NPs during the *in-situ* TEM heating from room temperature up to 900 °C.

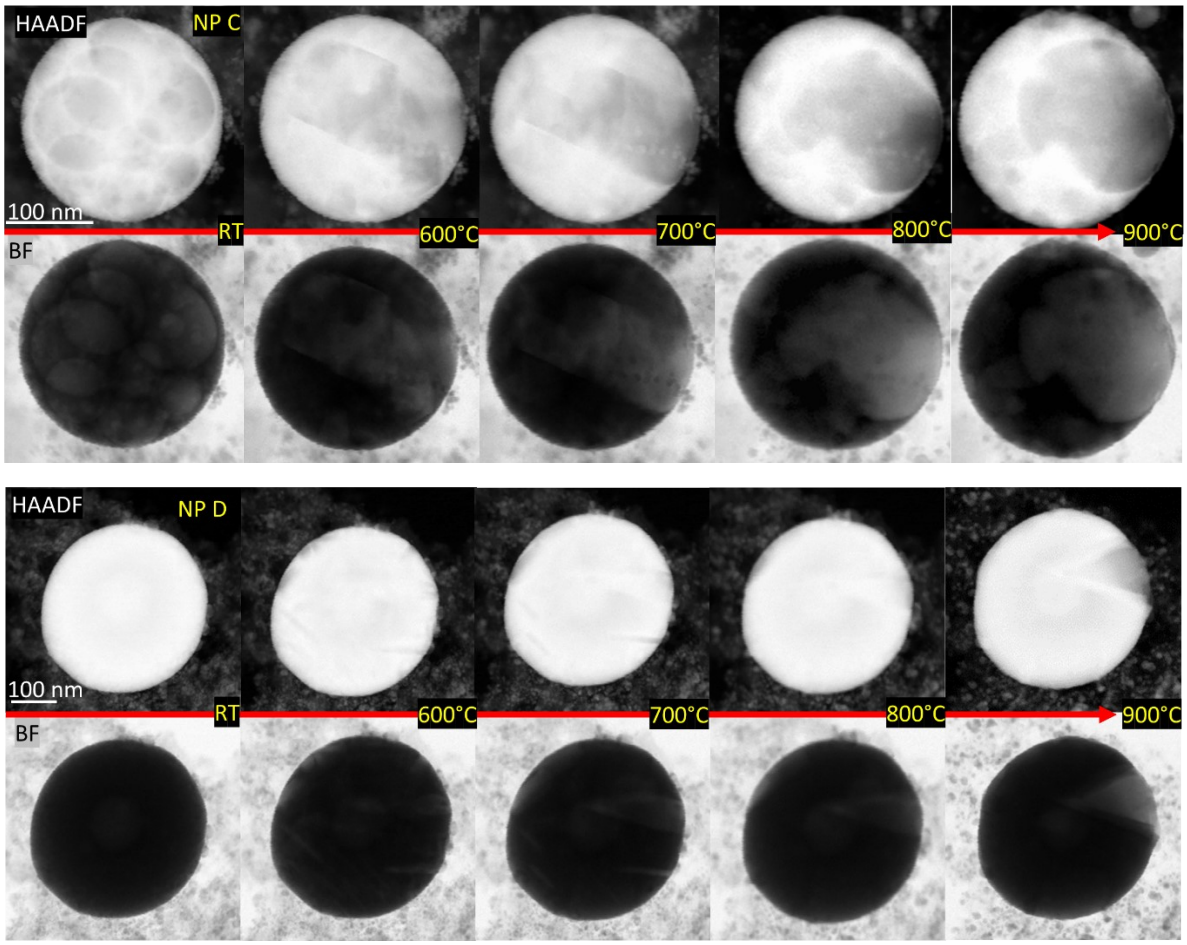

Figure S13. HAADF and BF STEM images showing the structure evolution of other two selected (Fe,Au) NPs during the *in-situ* TEM heating from room temperature up to 900 °C.

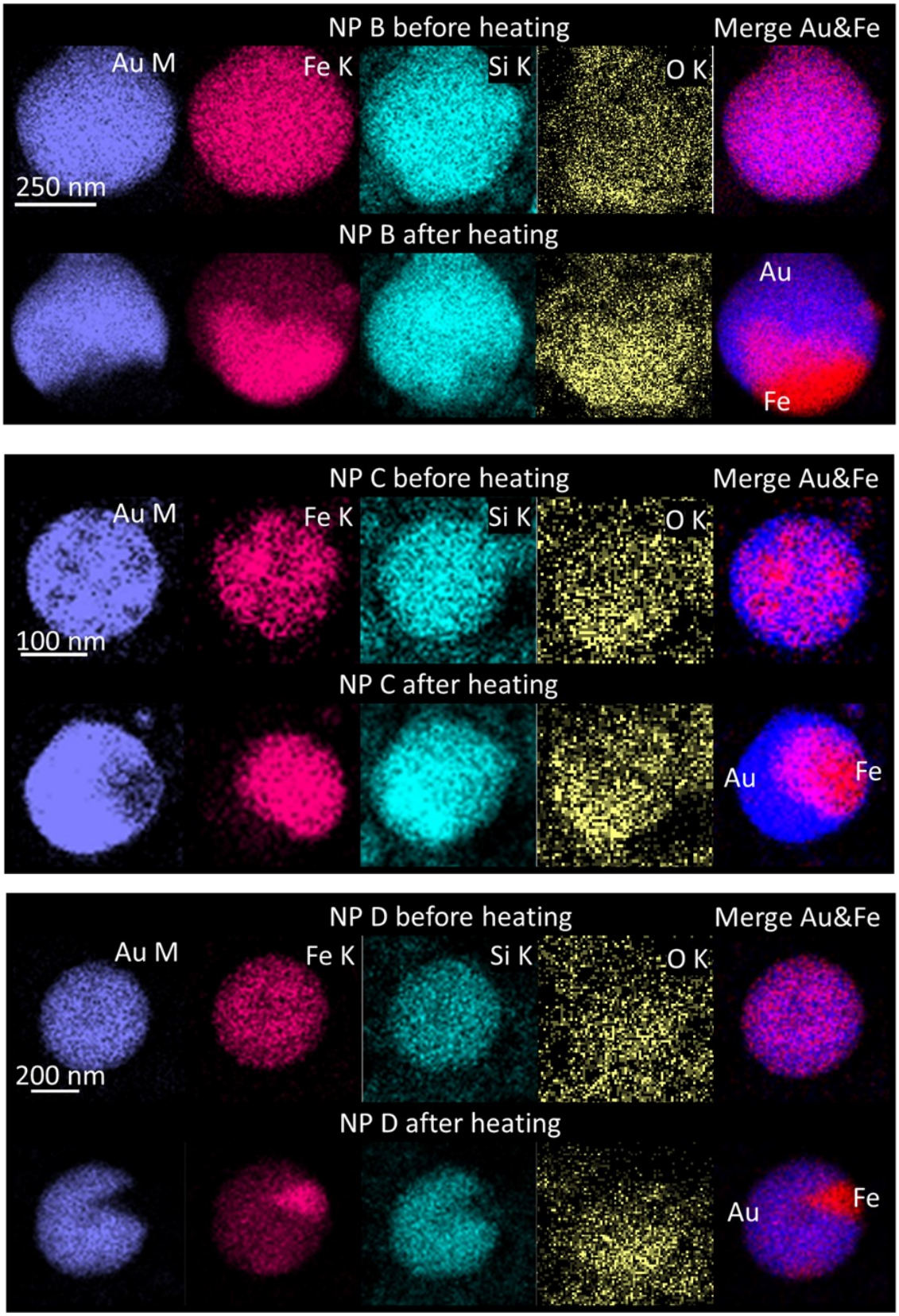

Figure S14. EDS elemental mapping image of the selected NPs before and after *in-situ* TEM heating from room temperature up to 900°C. Silicon is the contamination of the NPs, appeared during the EDDL process.

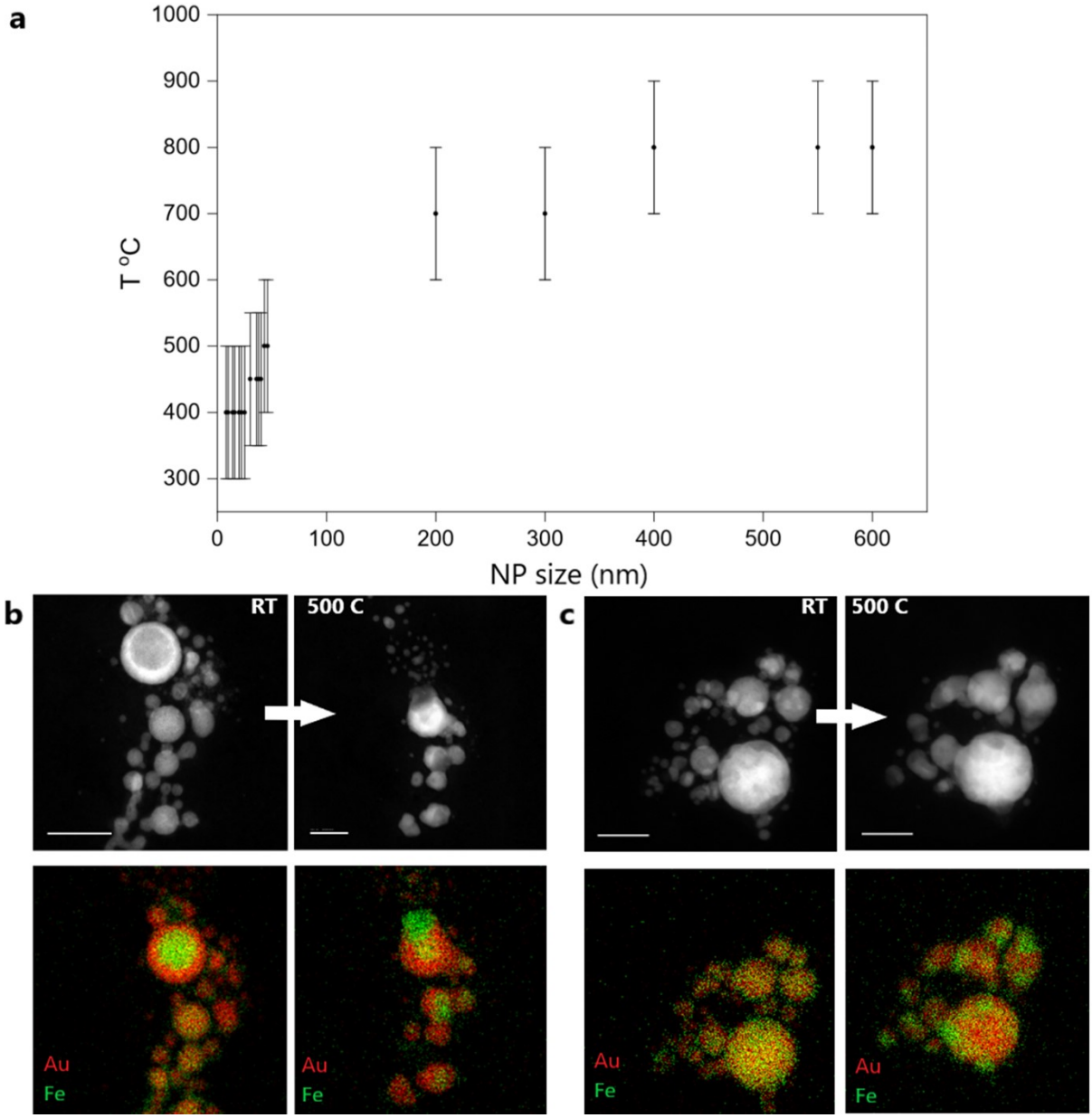

Figure S15. (a) Dependance of the transformation temperature on the NP size, obtained by *in situ* TEM analysis with heating mode. (b,c) The transformation of homogeneous metastable solid solution phase of the (Fe,Au) NP of 20 nm size towards an equilibrium biphasic Janus-type NP. Scale bar, 20 nm.

Part VI. Numerical modeling

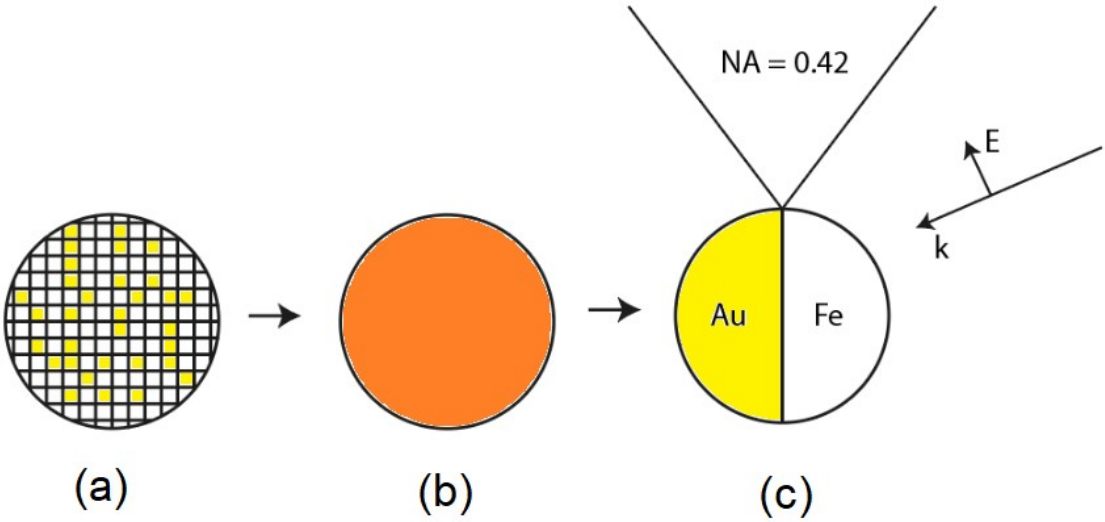

Figure S16. (a) Initial (Fe,Au) NPs represented as a random mixture of small Fe and Au clusters. (b) Corresponding effective dielectric permittivity of initial (Fe,Au) NP, obtained using Lorentz-Lorenz relation. (c) The NP after laser heating: Yellow - Au domain, White - Fe domain.

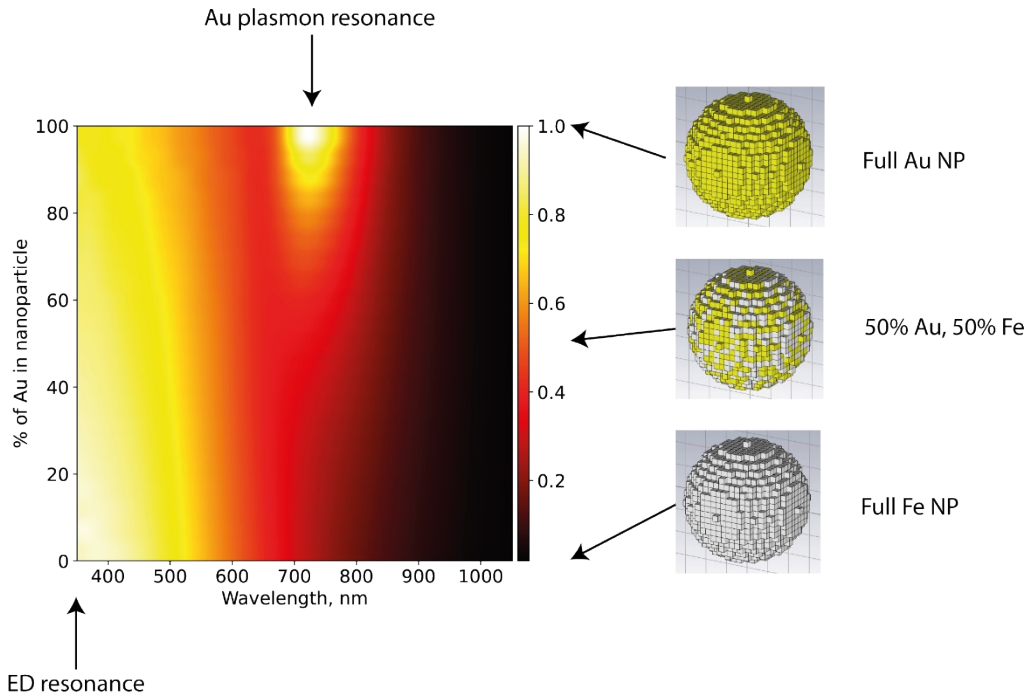

Figure S17. Dependence of fraction Au and Fe portions in NP on total scattering.

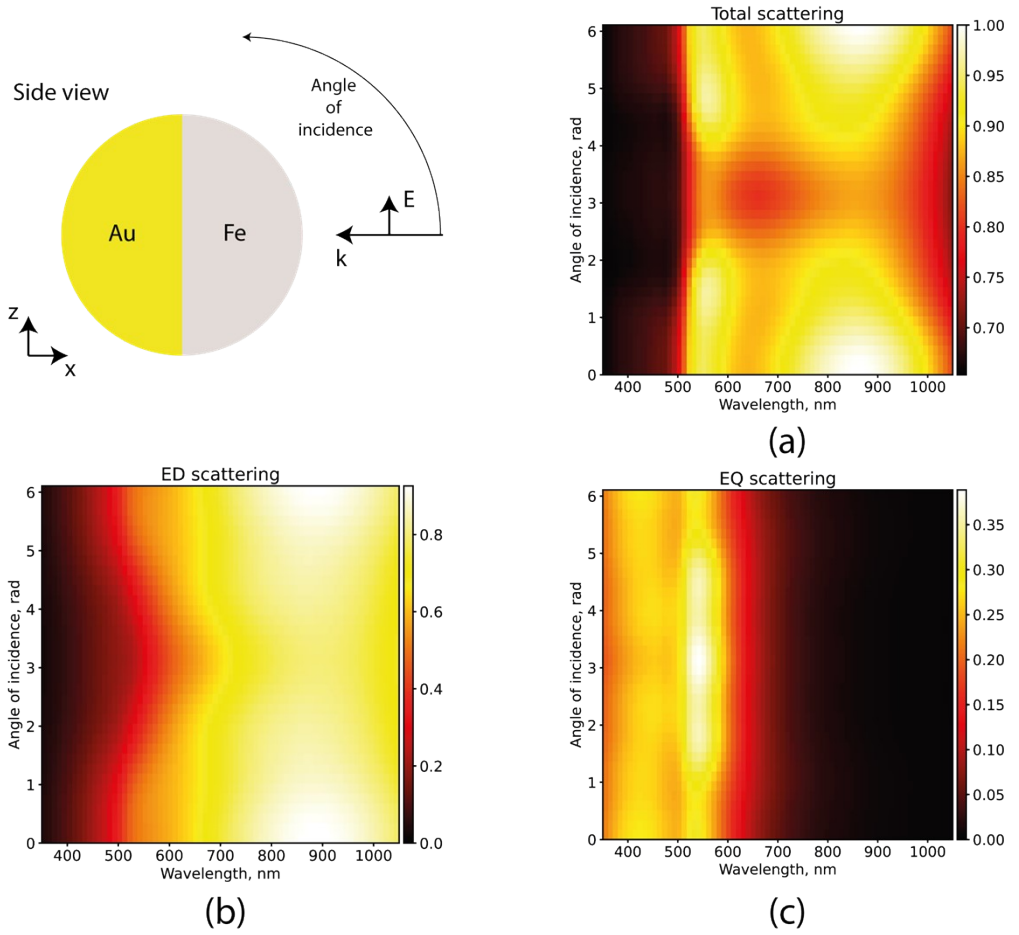

Figure S18. Total scattering of 50%-Au 50%-Fe NP for different angles of incidence.

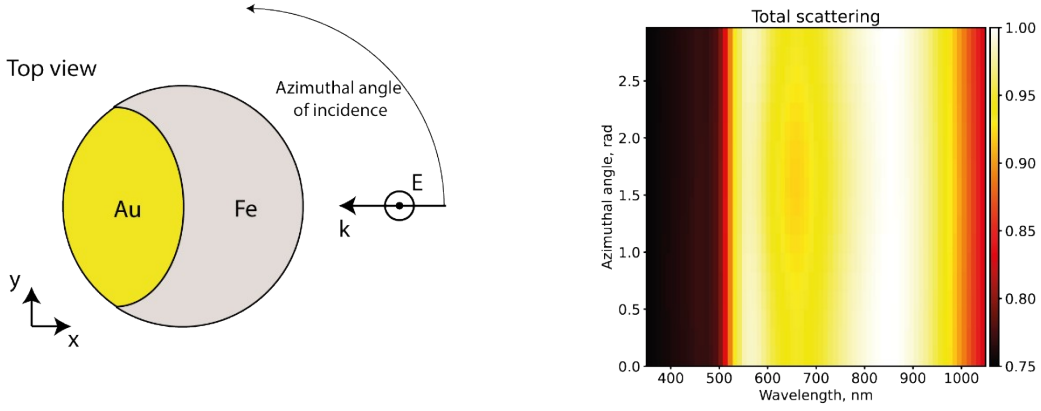

Figure S19. Total scattering of 50%-Au 50%-Fe NP for different azimuthal angles for 65° rotated particle.

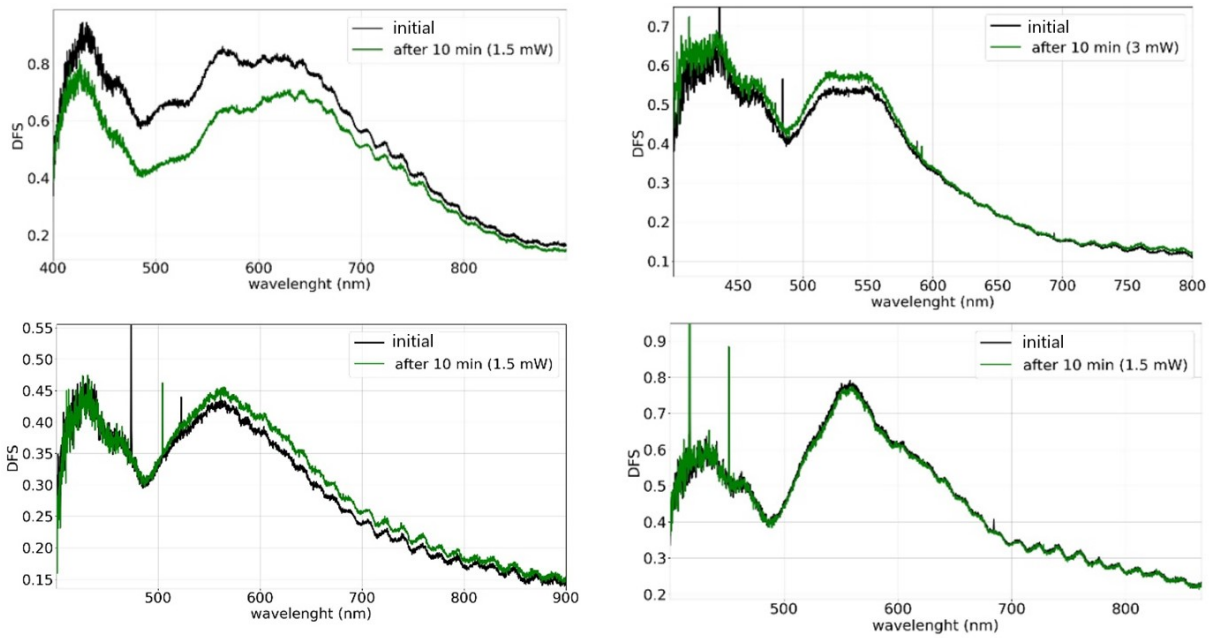

Figure S20. Statistical analysis of the effect of the heating (by light, 350 nm, 1.5 to 3 mW of the integral power) on the change of the light scattering spectrum for the (Fe,Au) NPs of different size and arbitrary element concentration (obtained in N_2 atmosphere), confirming that the concept of controlling the light scattering through the NP transformation is valid for diverse (Fe,Au) NPs.